# Electromagnetic Model of a Planar Radial-Waveguide Divider/Combiner Incorporating Probes

Marek E. Bialkowski, *Senior Member, IEEE,* and Vesa P. Waris, *Student Member, IEEE*

***Abstract*— A field matching technique is used to develop an electromagnetic model for an $M$-way planar radial-waveguide divider/combiner incorporating probes. Based on this model, a broadband operation of the radial divider/combiner is investigated. The application of the developed model is shown in a design example of a 20-way power divider.**

## I. Introduction

MICROWAVE power combiners/dividers are frequently used in microwave systems in which power division or combination is required. They play a vital role in the competition of solid-state power amplifiers with their counterparts—tube amplifiers. Many times in the past, waveguide transmission-line combiners, including rectangular, coaxial, conical, and radial [1]–[6], have been used, but only a few have been modeled so far. Most of the developed models are of the qualitative type, as they give only a general ideal of the waveguide combiner/divider operation. Quantitative models based on a full-wave analysis have been obtained only for rectangular waveguide combiners of the Kurokawa type [2], [3].

This paper reports on a full wave analysis of a planar radial-waveguide power combiner/divider which incorporates probes. Based on this analysis, an electromagnetic model of the device is obtained. This model is used to study the optimal dimensions of the radial power divider for its broadband operation.

## II. Formulation

Fig. 1 shows the configuration of the analyzed radial power divider/combiner. The device consists of a cylindrical cavity with one central probe and $M$ equispaced identical peripheral probes. The probes are formed by conducting posts, loaded with discs at their ends. For symmetry reasons, peripheral probes are assumed to be identical in shape and size. The central probe dimensions may differ from those of the peripheral probes. The probes are energized from gaps in the posts which are located between the cavity floor and the discs.

In practice, the probes may also be energized from coaxial entries, as shown in Fig. 1(c), diagram (i). However, since there exists an equivalence between the excitation from the coaxial entry and the gap in the post [12], there is no need to consider two types of excitation separately. In the theoretical approach, the coaxial entry of Fig. 1(c) (i) is replaced by an equivalent gap of Fig. 1(c) (ii). Note that the power divider/combiner described in the form above is regarded as a passive device. Active devices, if required, can be attached from the outside. To include active devices (i.e., Impatt or Gunn diodes), the probe configuration needs

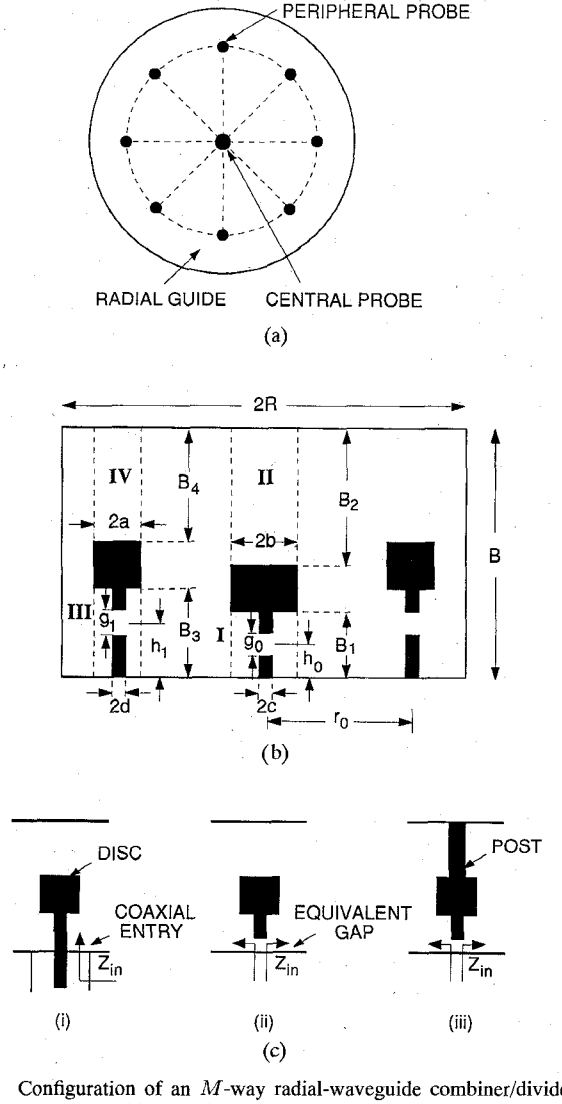


Fig. 1. Configuration of an $M$-way radial-waveguide combiner/divider incorporating probes. (a) top view, (b) side view (c) probe configurations: (i) probe energized from a coaxial line, (ii) probe energized from an equivalent gap in the post, (iii) probe suitable in the design of active power combiner.

Manuscript received March 3, 1992; revised October 16, 1992.

The authors are with the Department of Electrical Engineering, The University of Queensland, Queensland 4072, Australia.

IEEE Log Number 9209330.

to be modified from the one shown in Fig. 1(c) (i) to the one shown in Fig. 1(c) (iii). From a theoretical point of view, this modification is easy to accommodate. The required modification is explained in further analysis while producing the expressions for the fields in regions surrounding the probes.

The ideal operation of the passive power combiner/divider can be described as follows. In the power divider mode, the power is fed to the central probe and is equally divided without any loss between the match-terminated peripheral probes. In the power combiner mode, the power is fed in-phase to the peripheral probes and is collected without any loss by the match-terminated central probe. It is apparent that the ideal operation calls for the impedance match of the central and peripheral probes. This match can be obtained by choosing proper dimensions of the central and peripheral probes, and of the cavity.

To investigate the broadband match conditions, a full-wave analysis of this device is performed. An alternative analysis, which includes approximations of the sectorial guide containing the peripheral probe by a rectangular waveguide, is described in [13].

The present analysis is confined to the cases when the peripheral probes are fed in-phase or terminated in the same loads. To analyze the power divider/combiner, the admittance— rather than the scattering—matrix approach is chosen (no need for specifying characteristic impedances). However, once the admittance matrix parameters are known, conversion to the scattering parameters is straightforward.

For the case when the peripheral probes are fed in the same way or are terminated in identical loads, the admittance matrix parameters of the device are defined by the following equations

$$\begin{aligned} I_0 &= Y_{00}V_0 + (Y_{01} + \cdots + Y_{0M})V_1 \\ I_1 &= Y_{10}V_0 + (Y_{11} + \cdots + Y_{1M})V_1 \end{aligned} \tag{1a}$$

which can be rewritten in the form

$$\begin{aligned} I_0 &= Y_{00}V_0 + MY_{01}V_1 \\ I_1 &= Y_{10}V_0 + YY_{11}V_1 \end{aligned} \tag{1b}$$

where $V_0$ is the voltage applied in the gap #0 (in the central probe), $V_1$ is the voltage applied in the gap #1 (in the peripheral probes), and $I_0$, $I_1$ are the resulting currents in gaps #0 and #1.

Note that $YY_{11}$ in (1b) is given as the sum of $Y_{11}$, $Y_{12}, \cdots, Y_{1M}$. Equations (1a) and (1b) show that in order to obtain the admittance matrix for the symmetric radial power combiner/divider for the case when the peripheral probes are loaded or energized identically, two field problems have to be solved: 1) when the central probe is energized by voltage $V_o$ and the peripheral probes are short-circuited; and 2) when the peripheral probes are energized by the same voltage $V_1$ and the central probe is short-circuited.

Assuming that the parameters $Y_{00}$, $Y_{10}$ $Y_{01}$, and $YY_{11}$ are found, the input admittance seen at the central probe can be determined by using standard circuit analysis.

The problem becomes more complicated when the peripheral probes are energized or terminated arbitrarily. In this case, all the individual admittance matrix elements $Y_{11}$, $Y_{12}, \cdots, Y_{1M}$ in (1a), rather than their sum $YY_{11}$, have to be determined. This can be accomplished by solving the field problem for the situation when probe #1 is energized by voltage $V_1$ and all the remaining probes inside the cavity are short-circuited. Since expressions describing the interactions between the individual probes are derived in the Appendix for an arbitrary location and excitation, the extension of the present theory to this general case should be straightforward. The only new complication is the increased number of unknowns (namely, the number of expansion coefficients describing the local fields surrounding the peripheral probes) to be determined. This complication can, however, be overcome by solving $M$ problems exhibiting $M$-fold axial symmetry for which the number of unknowns can be reduced. These problems are defined by the conditions that the central probe is short-circuited and the peripheral probes $k = 1, \cdots, M$ are excited by voltages $V_{kp} = \exp(i\phi_o(k-1)(p-1))$, where $\phi_o = 360 \text{ deg}/M$ and $p = 1, \cdots, M$. Note that the sum of $V_{kp}$ versus $p$ divided by $M$ is equal to 1 only for $k = 1$ and otherwise is equal to 0. It is apparent that the superposition of the solutions to the new problems is equivalent to the solution of the initial problem with only one peripheral probe excited. The extension of the present theory to this case is not considered here but is a subject of further investigations in [14], [16].

For the peripheral probes terminated in identical loads characterized by the admittance $Y_L$, the input admittance at the central probe $Y_{in}$ is given by

$$Y_{in} = Y_{00} - MY_{01}Y_{10}/(YY_{11} + Y_L). \tag{2}$$

Having determined the input admittance, the input reflection coefficient at the central probe, with respect to an arbitrary characteristic admittance $Y_{c1}$, can easily be determined and is given by

$$T_{in} = -(Y_{in} - Y_{c1})/(Y_{in} + Y_{c1}). \tag{3}$$

From the earlier discussion of the ideal operation of the power combiner/divider, it is apparent that for the perfect combiner/divider, $T_{in}$ has to be zero for the case when the peripheral probes are terminated in their characteristic admittances $Y_{c2}$.

## III. Analysis

Currents $I_0$ and $I_1$ necessary to determine circuit parameters $Y_{ik}$, and therefore the value of $T_{in}$ in (3), can be obtained by using the relationship between the surface currents and the magnetic fields surrounding the probes. $I_0$ and $I_1$ are related to the magnetic field tangential components at the surfaces enclosing gaps #0 and #1 and are given by expressions [7]

$$\begin{aligned} I_0 &= \frac{1}{g_0}\frac{1}{2\pi}\int_{h_0-g_0/2}^{h_0+g_0/2}\int_0^{2\pi} H_\phi(r=c,y,\phi)\,d\phi\,dy \\ I_1 &= \frac{1}{g_1}\frac{1}{2\pi}\int_{h_1-g_1/2}^{h_1+g_1/2}\int_0^{2\pi} H_{\phi 1}(r_1=d,y,\phi)\,d\phi_1\,dy. \end{aligned} \tag{4}$$

The required magnetic field components in (4) can be determined by solving a suitably defined field problem for the divider/combiner.

It will be assumed that the field in the cavity is due to the uniform electric field $Ey = -V_0/g_0$, applied to the surface enclosing the gap #0 in the central probe, and the uniform electric field $Ey = -V_1/g_1$ applied to the surface enclosing gap #1 in the peripheral probes.

To determine the field in the cavity, a field matching technique can be used. To apply this technique, the entire cavity structure is divided into a number of cylindrical volumes: a cylindrical volume of radius $b$ surrounding the central probe, $M$ cylindrical volumes of radius $a$ surrounding the peripheral probes, and a cavity region outside the cylindrical volumes containing the probes.

The cylindrical volume containing the central probe is further divided into a cylindrical volume I below the disc, and volume II above the disc. Similarly, each cylindrical volume containing a peripheral probe is divided into a cylindrical volume III below the disc, and volume IV above the disc.

It is assumed that the individual cylindrical volumes, introduced above, can be filled with different uniform dielectrics, characterized by the dielectric constants $\epsilon_1$, $\epsilon_2$. $\epsilon_3$, $\epsilon_4$ for volumes I, II, III, and IV, for $\epsilon$ for the cavity region, respectively.

In the next step of the field matching procedure, it is required to write general expressions for the fields in volumes I, II, III, IV and match the tangential components of these fields to the cavity field, at the common cylindrical boundaries $r = b$ and $r_1 = a$.

The field components inside the volumes I, II, III, IV can be considered as internal, and those outside these volumes can be considered as external.

In order to simplify the analysis, the fields in the vicinity of the central and peripheral probes will be approximated by axially symmetric fields. This approximation should produce reasonably accurate results for the probes having dimensions $a$ and $b$ much smaller than the wavelength.

The approximation of the actual local field by an axially symmetric field implies that the $y$-component of the electric field and the $\phi$-component of the magnetic field are the only tangential components of the electromagnetic field at the cylindrical surfaces $r = b$ and $r_1 = a$. Therefore, in further analysis, only expressions for these two components are derived.

### A. Field Expansions—Probe Regions

Expressions for the fields in volumes I, II, III, IV can be obtained by following the analysis in [7]–[9]. Note, however, that as opposed to [7], volumes II and IV do not contain posts. Therefore, to describe the fields in volumes II and IV, new functions have to be introduced.

Following the analysis in [7], and by introducing the required modifications, the $y$-component of the electric field and the $\phi$-component of the magnetic field can be shown to be given by

$$
\begin{aligned}
E_y^I &= \sum_{n=0}^{\infty} \frac{\varepsilon_{on}}{B_1} \cos\left(k_{yn}^{(1)} y\right) \\
&\quad \cdot \left[ D1_n HJ\left(\Gamma_n^{(1)}, r, b, c\right) + E1_n HH\left(\Gamma_n^{(1)}, r, c\right) \right] \\
H_\phi^I &= \sum_{n=0}^{\infty} \frac{\varepsilon_{on}}{B_1} \cos\left(k_{yn}^{(1)y}\right) \frac{-jk_1}{Z_1 \Gamma_n^{(1)}} \\
&\quad \cdot \left[ D1_n HJP\left(\Gamma_n^{(1)}, r, b, c\right) + E1_n HHP\left(\Gamma_n^{(1)}, r, b\right) \right] \\
E_y^{II} &= \sum_{n=0}^{\infty} \frac{\varepsilon_{on}}{B_2} \cos\left(k_{yn}^{(2)}(y - B_2)\right) D2_n JJ\left(\Gamma_n^{(2)}, r, b\right) \\
H_\phi^{II} &= \sum_{n=0}^{\infty} \frac{\varepsilon_{on}}{B_2} \cos\left(k_{yn}^{(2)}(y - B_2)\right) \frac{-jk_2}{Z_2 \Gamma_n^{(2)}} \\
&\quad \cdot D2_n JJP\left(\Gamma_n^{(2)}, r, b\right)
\end{aligned} \tag{5}
$$

where

$$
HJ\left(\Gamma_n^{(1)}, r, b, c\right) = \frac{H_o^{(2)}\left(\Gamma_n^{(1)} r\right) J_0\left(\Gamma_n^{(1)} c\right) - J_0\left(\Gamma_n^{(1)} r\right) H_0^{(2)}\left(\Gamma_n^{(1)} c\right)}{H_1^{(2)}\left(\Gamma_n^{(1)} r\right) J_0\left(\Gamma_n^{(1)} c\right) - J_1\left(\Gamma_n^{(1)} b\right) H_0^{(2)}\left(\Gamma_n^{(1)} c\right)}
$$

$$
HH\left(\Gamma_n^{(1)}, r, c\right) = \frac{H_0^{(2)}\left(\Gamma_n^{(1)}, r\right)}{H_o^{(2)}\left(\Gamma_n^{(1)}, c\right)},
$$

$$
JJ\left(\Gamma_n^{(2)}, r, b\right) = \frac{J_0\left(\Gamma_n^{(2)} r\right)}{J_1\left(\Gamma_n^{(2)} b\right)}
$$

$(k_1, Z_1)$, $(k_2, Z_2)$ are the wave number and the intrinsic impedance for volumes I, II.

$$
HJP\left(\Gamma_n^{(1)}, r, b, c\right) = \frac{\partial HJ\left(\Gamma_n^{(1)}, r, b, c\right)}{\partial\left(\Gamma_n^{(1)} r\right)},
$$

$$
HHP\left(\Gamma_n^{(1)}, r, c\right) = \frac{\partial HH\left(\Gamma_n^{(1)}, r, c\right)}{\partial\left(\Gamma_n^{(1)} r\right)}
$$

$$
JJP\left(\Gamma_n^{(2)}, r, b\right) = \frac{\partial JJ\left(\Gamma_n^{(2)}, r, b\right)}{\partial\left(\Gamma_n^{(2)} r\right)}
$$

$$
k_{yn}^{(1)} = \frac{n\pi}{B_1}, \quad k_{yn}^{(2)} = \frac{n\pi}{B_2} \text{ are eigenvalues},
$$

$$
\Gamma_n^{(1)^2} = k_1^2 - y_{yn}^{(1)^2},
$$

$$
\Gamma_n^{(2)^2} = k_2^2 - k_{ym}^{(2)^2}, J_0 H_0^{(2)}, J_1, H_1^{(2)}
$$

are Bessel and Hankel function of 0th and 1st order, $\epsilon_{on}$ is the Neumann factor.

$$
E1_n = V_0 \cos\left(k_{yn}^{(1)} h_1\right) \sin\left(k_{yn}^{(1)} g_1/2\right) \Big/ \left(k_{yn}^{(1)} g_1/2\right)
$$

are expansion coefficients for the electric field $E_y = -V_0/g_0$ in the gap #0. $D1_n$, $D2_n$ in (5) are the field expansion coefficients, yet to be determined.

Expressions for the fields in volumes III and IV can be obtained by introducing the following substitutions in expressions (5):

$$B_1 \to B_3, \quad B_2 \to B_4, \quad b \to a, \quad c \to d, \quad g_0 \to g_1,$$
$$h_0 \to h_1, \quad k_1 \to k_3, \quad k_2 \to k_4, \quad Z_1 \to Z_3, \quad Z_2 \to Z_4,$$
$$k_{yn}^{(1)} \to k_{yn}^{(3)}, \quad k_{yn}^{(2)} \to k_{yn}^{(4)}, \quad \Gamma_n^{(1)} \to \Gamma_n^{(3)}, \quad \Gamma_n^{(2)} \to \Gamma_n^{(4)},$$
$$E1_n \to E3_n, \quad D1_n \to D3_n, \quad D2_n \to D4_n.$$

The above-derived expressions for the field components are valid for the case when the probes are of type (ii) [Fig. 1(c)] with empty regions above the discs. These expressions, however, can easily be extended for the case of probe type (iii) [Fig. 1(c)] with the post above the disc. The required modifications are straightforward. To include the post in the region above the disc, the functions $JJ$ and $JJP$ describing the $y$-component of the electric field and the $\phi$-component of the magnetic field in regions II and IV have to be replaced by functions $HJ$ and $HJP$, respectively.

### B. Field Expansions—External Region

To determine the external tangential field components at the interfaces $r = b$ and $r_1 = a$, expressions for the electric and magnetic fields due to a single, arbitrarily positioned probe in a radial cavity, derived in the Appendix, can be used. Now, those expressions have to be extended to the case of $M$ symmetrically positioned peripheral probes and one central probe. To simplify derivations, it is assumed that one of the peripheral probes is positioned at $r = r_0$, $\phi = 0$. In this case, the combiner/divider configuration becomes symmetric with respect to $\phi = 0$, and for the assumed type of excitation the fields become even functions of $\phi$. As a result, the exponential terms $\exp(-jp\phi)$ in the azimuthal expansions for the electric magnetic field components (A6), (A7) are replaced by $\cos(p\phi)$ terms.

The other modification comes from the $M$-fold symmetry of the divider/combiner. Because of the $M$-fold symmetry of the device and its excitation, all the azimuthal harmonics in expressions for the electric and magnetic fields inside the radial cavity which do not exhibit the $M$-fold symmetry disappear. This implies that in the term $Qn$, which appears in expressions (A8)–(A11), only harmonics of the order $p = 0, M, 2M$, etc., have to be retained.

Having exploited all the symmetries of the radial combiner/divider, derivations for the expressions for the $y$-component of the electric field and the $\phi$-component of the magnetic field at the cylindrical boundaries $r = b$ and $r_1 = a$ become straightforward.

For the central probe (at $r = b$),

$$Ey = \sum_{n=0}^{\infty} \frac{\epsilon_{on}}{B} [A_n UU(n) + C_n VV(n)] \cos(k_{yn} y)$$
$$H\phi = \sum_{n=0}^{\infty} \frac{\epsilon_{on}}{B} \frac{-jk}{Z_0 \Gamma_n} [A_n UUP(n) + C_n VVP(n)] \cos(k_{yn} y) \tag{6}$$

where $k$, $Z_0$ are the wave number and intrinsic impedance for the cavity region outside the cylindrical volumes containing the probes. The remaining symbols are defined as follows:

$$UU(n) = H_0^{(2)}(\Gamma_n b) - J_0(\Gamma_n b) H_0^{(2)}(\Gamma_n R)/J_0(\Gamma_n R),$$
$$VV(n) = M J_0(\Gamma_n b) P_n$$
$$P_n = H_0^{(2)}(\Gamma_n r_0) - J_0(\Gamma_n r_0) H_0^{(2)}(\Gamma_n R)/J_0(\Gamma_n R),$$
$$UUP(n) = \frac{\partial UU(n)}{\partial(\Gamma_n b)}, \quad VVP(n) = \frac{\partial VV(n)}{\partial(\Gamma_n b)}$$
$$\Gamma_n^2 = k^2 - k_{yn}^2, \quad k_{yn} = \frac{n\pi}{B}.$$

For the peripheral probe (at $r_1 = a$),

$$Ey = \sum_{n=0}^{\infty} \frac{\epsilon_{on}}{B} [A_n TT(n) + C_n QQ(n)] \cos(k_{yn} y)$$
$$H\phi_1 = \sum_{n=0}^{\infty} \frac{\epsilon_{on}}{B} \frac{-jk}{Z_0 \Gamma_n} [A_n TTP(n) + C_n QQP(n)] \cos(k_{yn} y) \tag{7}$$

where

$$TT(n) = J_0(\Gamma_n a) P_n, \qquad QQ(n) = J_0(\Gamma_n a) Q_n + H_0^{(2)}(\Gamma_n a)$$
$$TTP(n) = \frac{\partial TT(n)}{\partial(\Gamma_n a)}, \qquad QQP(n) = \frac{\partial QQ(n)}{\partial(\Gamma_n a)}$$

where $Q_n$, defined in the Appendix, is now modified to the following form:

$$Q_n = \sum_{m=2}^{M} H_0^{(2)}(\Gamma_n r_{m1}) - M \sum_{p=0,M,2M}^{\infty} \epsilon_{op} J_p^2(\Gamma_n r_0) H_p^{(2)}(\Gamma_n R)/J_p(\Gamma_n R)$$

where $r_{m1}$ is the distance between the middle positions of the 1st probe and the $m$th probe.

### C. Field Matching

The remaining goal in the field matching procedure is the determination of the field expansion coefficients. For this purpose, continuity conditions for the tangential field components are used. These conditions can be stated by the following equations.

At $r = b$,

$$E_{y(ext)} = \begin{cases} Ey^I & 0 \le y \le B_1 \\ 0 & \text{for } B_1 \le y \le B - B_2 \\ Ey^{II} & B - B_2 \le y \le B \end{cases}$$
$$H_\phi^I = H_{\phi(ext)} \quad \text{for } 0 \le y \le B_1,$$
$$H_\phi^{II} = H_{\phi(ext)} \quad \text{for } B - B_2 \le y \le B. \tag{8}$$

Similarly, at $r_1 = a$,

$$H_\phi^{III} = H_{\phi(ext)} \quad \text{for } 0 \le y \le B_3$$
$$H_\phi^{IV} = H_{\phi(ext)} \quad \text{for } B - B_4 \le y \le B$$
$$E_{y(ext)} = \begin{cases} Ey^{III} & 0 \le y \le B_3 \\ 0 & \text{for } B_3 \le y \le B - B_4 \\ Ey^{IV} & B - B_4 \le y \le B. \end{cases} \tag{9}$$

Equations (8) and (9) are in the functional form and are therefore unsuitable for computations.

In order to convert (8) and (9) into algebraic equations, which can be handled by a computer, the following integrations are performed.

At $r = b$,

$$\int_0^B Ey_{(ext)} \cos(k_{yl} y)\, dy = \int_0^{B_1} Ey^1 \cos(k_{yl} y)\, dy + \int_{B-B_2}^{B} Ey^{II} \cos(k_{yl} y)\, dy \qquad l = 0, 1, \cdots$$

$$\int_0^{B^1} H_\phi^I \cos\left(k_{ym}^{(1)} y\right) dy = \int_0^{B^1} H_{\phi(ext)} \cos\left(k_{ym}^{(1)} y\right) dy \qquad m = 0, 1, \cdots$$

$$\int_{B-B_2}^{B} H_\phi^{II} \cos\left(k_{yp}^{(2)}(y-(B-B_2))\right) dy = \int_{B-B_2}^{B} H_{\phi(ext)} \cdot \cos\left(k_{yp}^{(2)}(y-(B-B_2))\right) dy \qquad p = 0, 1, \cdots . \tag{10}$$

At $r_1 = a$, the required integrations are analogous to those at $r = b$, shown in (10). The necessary changes are obtained by replacing indices 1, 2 in (10), corresponding to volumes I, II, with new indices 3, 4 corresponding to volumes II, IV.

## IV. Results

Based on the theory described above a computer algorithm in MICROSOFT Fortran for an IBM PC for the analysis of an $M$-way radial waveguide divider/combiner was developed. This algorithm was aimed at calculating the input admittance (2) as observed at the central probe for the case when the peripheral probes were loaded identically. In calculations, infinite expansions describing the fields in individual volumes I, II, III, and IV and the cavity region were truncated. To evaluate 0th and 1st-order Bessel and Neumann functions, polynomial approximations [11] were used. Higher order Bessel and Neumann functions were evaluated by using recursion formulas [11]. For Bessel functions, the backward recursion formula was used. For Neumann functions, the forward recursion formula was applied.

In order to test the developed theory, and especially the validity of the approximation that the actual fields in regions I, II, III, and IV surrounding the probes are axially symmetric fields, a two-probe divider was built. The device included a radial cavity with one central probe and one peripheral probe. For this device, a comparison between experimental and theoretical results for the scattering parameters $S_{00}$ (reflection coefficient of the central probe) and $S_{11}$ (reflection coefficient of the peripheral probe) could be performed.

Fig. 2 shows a comparison between theoretical and experimental values for $S_{00}$ and $S_{11}$ in the frequency band from 8 to 12 GHz. Experimental results were obtained by using probes (type (i) of Fig. 1(c)] fed from 50 Ω coaxial lines. The reference plane for measurements was chosen at the junction between the coaxial line and the radial cavity. A Hewlett-Packard vector network analyzer HP 8510 B was used in the measurements. Numerical results were obtained by using the "equivalent gap" approach [see Fig. 1(c) (ii)]. In the latter case, results for $S_{00}$ and $S_{11}$ were referenced to the cylindrical surface enclosing the gap. Although good agreement was obtained between the measured and calculated reflection coefficient for both the central and the peripheral probe, the numerical results for the central probe seem to be in slightly better agreement with experimental data. This can be explained by the fact that the region which surrounds the central probe exhibits a better axial symmetry than the one which surrounds the peripheral probe.

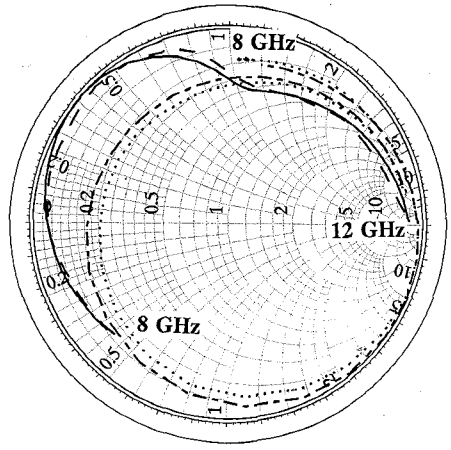


Fig. 2. Comparison between theoretical and experimental results for the scattering parameters $S_{00}$ and $S_{11}$ of the two-probe divider. Dimensions: radial cavity $R = 19.5$ mm, $B = 6.75$ mm, central probe $d = 0.65$ mm, $b = 2.3$ mm, $B_1 = 1.65$ mm, $B_2 = 1.10$ mm, $g_0 = B_1$, $h_0 = B_1/2$, peripheral probe $c = 0.65$ mm, $a = 2.2$ mm, $B_3 = 2.00$ mm, $B_4 = 1.60$ mm, $g_1 = B_3$, $h_1 = B_3/2$, $r_o = 13.5$ mm. Coaxial probe outer conductor radius 2.1 mm. $S_{00}$: theory ———, experiment - - -, $S_{11}$: theory -.-.-, experiment ·····.

In the next step, the developed algorithm was applied to the design of a 20-way radial divider. By using the developed algorithm, a search for the device's optimal dimensions was initiated to produce the maximum value of the return loss for the central probe, in the 10–18 GHz band. In the search, the initial dimensions were chosen as follows. In order to obtain the dominant mode propagation (uniform with height radial waves), the waveguide height was chosen to be less than a half-wavelength, at 18 GHz. Distances between adjacent peripheral probes were chosen approximately equal to half-free-space wavelength, at the middle frequency of 14 GHz. The distance between the peripheral probe and the cavity wall was chosen approximately equal to a quarter-wavelength, at the middle frequency of 14 GHz. It is worthwhile to mention that to produce 20 frequency points for the input impedance of the central probe, it took only several seconds of CPU time of 486DX/33MHz PC.

In order to validate the theoretical result, the actual model of the 20-way radial combiner/divider was built. This model incorporated coaxial probes which were energized from coaxial entries.

Figure 3 shows the final dimensions of the radial divider/combiner and a comparison between theoretical and

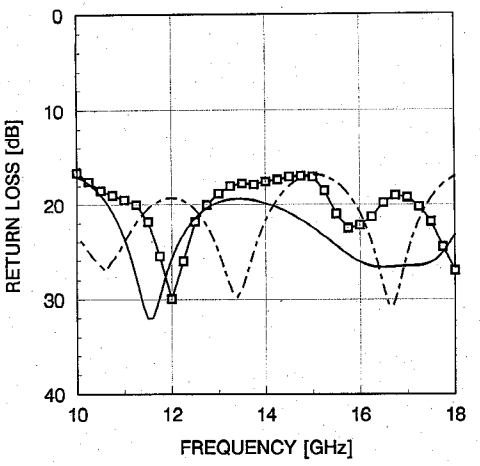


Fig. 3. Comparison between theoretical and experimental results for the return loss (referenced to 50 Ω) of the central probe in the 20-way redial divider. Radial cavity dimensions: $B = 5.5$ mm, $R = 39$ mm. Central probe dimensions: $c = 0.65$ mm, $b = 1.8$ mm, $B_1 = 1.45$ mm, $B_2 = 1.20$ mm, $g_0 = B_1$, $h_0 = B_1/2$. Peripheral probe dimensions: $d = 0.65$ mm, $a = 1.8$ mm, $B_3 = 2.1$ mm, $B_4 = 1.50$ mm, $g_1 = B_3$, $h_1 = B_3/2$. Peripheral probe position $r_o = 34.1$ mm.
Theory: peripheral probes terminated with 50 Ω loads _____, peripheral probes terminated with 43 Ω loads - - -, Experiment: o - - o - - o.

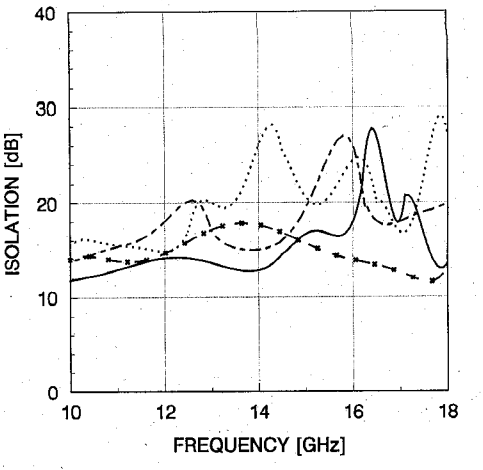


Fig. 4. Measured isolation in the 20-way radial divider. Isolation between probes: 20th and 1st _____, 20th and 2nd - - -, 20th and 5th _ _ _ _, 20th and 10th - - * - - * - - *.

experimental results for the values of the return loss observed at the central probe (for the case when the peripheral probes were terminated in 50 Ω loads). Both theoretical and experimental results show a reasonably good quality match, corresponding to the return loss of not worse than 17 dB throughout the entire band from 10 to 18 GHz.

The discrepancy between theoretical and experimental results can be explained by different reasons, such as approximations used in the theory or the difference in probe excitations. It was, however, felt that the more obvious reason would be the use of nonideal SMA match loads which terminated the peripheral probes during measurements.

To confirm this hypothesis, a separate set of measurements on SMA terminations was performed. These measurements showed that the return loss for individual SMA terminations ranged from 20 to 30 dB in the entire 10–18 GHz frequency band. In order to investigate the influence of nonideal match terminations, another set of calculations was performed. Fig. 3 shows the return loss observed at the central probe when the SMA loads are modeled by constant admittances of 43 Ω (this corresponds to 22.5 dB return loss).

It can be seen that, in the last case, the maximum value of the return loss did not change and was about 17 dB. However, the shape of the curve representing the return loss for the central probe had changed significantly. This simulation showed that indeed nonideal terminations are likely to be responsible for slight discrepancies between theoretical and experimental results for the return loss of the central probe.

In order to further test the design of the 20-way divider, isolation measurements in the 10–18 GHz band between selected probes were performed. Fig. 4 shows the experimental results for the isolation between the 20th and 1st, 2nd, 5th, and 10th probe, respectively. It can be seen that, on average, the isolation is better than 10 dB. The best isolation seems to be between the 20th and the 2nd probe (for the probes which are interleaved by one probe). The worst isolation is between the 20th and the 10th probe, (the probes located on the opposite sides of the divider).

## V. Conclusions

A field matching technique for the analysis of a planar radial-waveguide power combiner/divider has been presented. Based on this analysis, a computer algorithm for determining the admittance matrix parameters of the radial combiner/divider has been developed.

This algorithm was tested on the example of a two-probe device. Good agreement between theoretical and experimental results for the reflection coefficient of the central and the peripheral probe was noted. In the next step, the algorithm was used to determine the optimal dimensions of the 20-way power divider for its operation in the 10–18 GHz frequency band. The theoretical design was verified experimentally by building the physical model of the 20-way radial combiner/divider. Comparison of the results has shown good agreement between the developed theory and experiment. The analysis and computer algorithm described here should prove useful to the designers of radial-waveguide combiners/dividers in the future.

## Appendix

### *Cylindrical Cavity with a Single Probe*

Fig. 5 shows the top view of a radial cavity of radius $R$ and height $B$ containing two cylindrical regions of different radii $a$ and $b$ and of equal height $B$. Inside the cavity, there is a probe which energizes the entire structure. The probe is located inside a cylinder of radius $a$, which is positioned at $r = r_0$, $\phi = \phi_0$. It is assumed that the shape of the probe and the form of excitation are such that the probe supports an axially symmetric current having a $y$-component, possibly a radial $r_1$-component, and no $\phi_1$-component.

From the theory of cavities [10], [15], it is known that under the above-specified conditions, the field existing in the cavity is described in terms of radial TM (to the $y$-direction) waves.

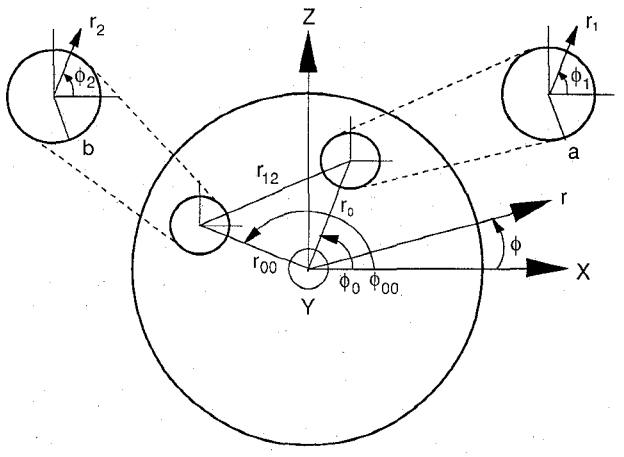


Fig. 5. Configuration of a radial cavity with three cylindrical coordinate systems used in the analysis of the fields radiated by an arbitrarily positioned probe.

In the analysis of the radial power combiner/divider, only the $y$-component of the electric field and the $\phi$-component of the magnetic field are required to be determined.

For convenience, three systems of coordinates—$r$, $\phi$, $y$—associated with the cavity, $r_1$, $\phi_1$, $y$, associated with the cylinder containing the probe, and $r_2$, $\phi_2$, $y$, associated with the second cylindrical volume of radius $b$, are introduced. The field produced by the probe in the cavity can be considered to be composed of two parts: 1) the field generated by the probe in the absence of the side cavity wall: and 2) the field scattered by the wall.

Let us assume that in the absence of the side cavity wall, the current flowing on the probe generates a wave whose $y$-component of the electric field is given by

$$E_{yn(inc)} = H_0^{(2)}(\Gamma_n r_1)\cos(k_{yn} y) \tag{A1}$$

where $H_0$ is the Hankel function

$$k_{yn} = \frac{n\pi}{B}, \quad \Gamma_n^2 = k^2 - k_{yn}^2 .$$

Note that $E_{yn(inc)}$ is a constant function of $\phi_1$ in the local coordinate system $r_1$, $\phi_1$, $y$, which is associated with the probe, but may vary with $\phi$ in the global coordinate system $r$, $\phi$, $y$, associated with the cavity.

When the cavity wall is introduced the radial wave generated by the probe is scattered by the cavity wall. Since $E_{yn(inc)}$ is nonsymmetric with respect to the cavity wall, the scattered field is formed by an infinite number of the $\phi$-harmonics traveling in toward the cavity's centre.

In order to determine the magnitude of these harmonics, $E_{yn(inc)}$ in (A1) is first rewritten in terms of global (cavity) coordinates $r$, $\phi$, $y$. The required conversion is obtained by using the addition theorem [11] for cylindrical functions. By using the addition theorem [11], $E_{yn(inc)}$ in (A1) can be written in the form

$$E_{yn(inc)} = \sum_{p=-\infty}^{\infty} e^{jp(\phi-\phi_0)} \begin{Bmatrix} J_p(\Gamma_n r_0) H_p^{(2)}(\Gamma_n r) \\ J_p(\Gamma_n r) H_p^{(2)}(\Gamma_n r_0) \end{Bmatrix} \cdot \cos(k_{yn} y) \tag{A2}$$

where upper row expansion is valid for $r \geq r_0 + a$, and lower row expansion is valid for $r \leq r_0 - a$, $H_p$ and $J_p$ are the $p$th-order Hankel and Bessel functions, respectively.

Since the scattered electric field is given by the sum of the empty cavity modes, the $y$-component $E_{yn(scat)}$ is represented by

$$E_{yn(scat)} = \sum_{p=-\infty}^{\infty} X_{pn} J_p(\Gamma_n r) e^{jp\phi} \cos(k_{yn} y) \tag{A3}$$

where $X_{pn}$ are expansion coefficients.

Coefficients $X_{pn}$ can be determined from the condition that the $y$-component of the total field $E_{yn(tot)} = E_{yn(inc)} + E_{yn(scat)} = 0$, on the side cavity wall, and are given by

$$X_{pn} = -J_p(\Gamma_n r_0) \frac{H_p^{(2)}(\Gamma_n R)}{J_p(\Gamma_n R)} e^{-jp\phi_0} . \tag{A4}$$

The $y$-component of the total field produced by the probe inside the cavity is obtained by combining (A1) and (A4) and is given by

$$E_{yn(tot)} = \left[ H_o^{(2)}(\Gamma_n r_1) + \sum_{p=-\infty}^{\infty} X_{pn} J_p(\Gamma_n r) e^{jp\phi} \right] \cdot \cos(k_{yn} y) \tag{A5}$$

where $X_{pn}$ are given by (A4).

The result, shown in (A5), is valid for the case when the $y$-component of the electric field varies with $y$ as $\cos(k_{yn} y)$.

To generalize (A5) for the case of an arbitrary variation of $Ey$ with $y$, an infinite sum of the $y$-harmonics (A5) has to be used. In this case, $Ey$ is given by

$$E_y = \sum_{n=0}^{\infty} C_n \frac{\epsilon_{on}}{B} \left[ H_o^{(2)}(\Gamma_n r_1) + \sum_{p=-\infty}^{\infty} X_{pn} J_p(\Gamma_n r) e^{jp\phi} \right] \cdot \cos(k_{yn} y) \tag{A6}$$

where $C_n$ are expansion coefficients, depending on the particular form of probe and its excitation. The $\phi$-component of the magnetic field produced by the probe can be determined from Maxwell's equations or alternatively by using the relationship which holds for TM radial wave harmonics [10]

$$H_{\phi n} = \frac{jk}{Z_o \Gamma_n^2} \frac{\partial E_{yn}}{\partial r}$$

and is given by

$$H_\phi = \sum_{n=0}^{\infty} C_n \frac{\epsilon_{on}}{B} \frac{jk}{Z_o \Gamma_n^2} \frac{\partial}{\partial r} \cdot \left[ H_o^{(2)}(\Gamma_n r_1) + \sum_{p=-\infty}^{\infty} X_{pn} J_p(\Gamma_n r) e^{jp\phi} \right] \cos(k_{yn} y) . \tag{A7}$$

*Averages of the Electric and Magnetic Fields Over Cylindrical Surfaces*

In the analysis of the radial power divider/combiner, it is required to extract from expressions (A6) and (A7) the axially symmetric terms of the $y$-component of the electric field and the $\phi_1$- and $\phi_2$-components of the magnetic field at two cylindrical surfaces: $r_1 = a$ and $r_2 = b$, respectively (Fig. 5).

The required axially symmetric terms can be obtained by applying the addition theorem to the cylindrical functions in (A6), (A7) and by retaining only symmetric (constant with $\phi$) terms in infinite expansions. By using this procedure, the following approximations of the fields are obtained.

For the cylindrical volume $r_1 \leq a$, inside which the probe is located, $E_y$ is approximated by

$$E_y(r_1 \cong a) = \sum_{n=0}^{\infty} \frac{\epsilon_{on}}{B} C_n \Big( Q_n J_0(\Gamma_n r_1) + H_0^{(2)}(\Gamma_n r_1) \Big) \cdot \cos(k_{yn} y)$$

where

$$Q_n = -\sum_{p=0}^{\infty} \epsilon_{op} J_p^2(\Gamma_n r_0) H_p^{(2)}(\Gamma_n R)/J_p(\Gamma_n R) . \quad \text{(A8)}$$

Note that in the expression (A8), the singular nature of the field is represented by the Hankel function

$$H_0^{(2)}(\Gamma_n r_{1i}) .$$

For $\Gamma_n^2 < 0$, radial waves produced by the peripheral probes decay with distance and therefore the expression for $Qn$ can be approximated by

$$Q_n = -H_0^{(2)}(\Gamma_n r_{1i})$$

where $r_{1i}$ is the distance between the middle position of the probe and its first image against the side cavity wall.

The $\phi_1$-component of the magnetic field for points inside the cylinder $r_1 \leq a$ can be approximated by

$$H_{\phi_1}(r_1 \cong a) = \sum_{n=0}^{\infty} \frac{\varepsilon_{on}}{B} \frac{jk}{Z_o \Gamma_n} C_n \cdot \Big( Q_n J_1(\Gamma_n r_1) + H_1^{(2)}(\Gamma_n r_1) \Big) \cos(k_{yn} y) . \quad \text{(A9)}$$

The axially symmetric terms for the $y$-component of the electric field and the $\phi_2$-component of the magnetic field at the cylindrical surface $r_2 = b$ can be obtained by using a similar procedure to that which used to obtain (A8) and (A9). Note, however, that as opposed to volume $r_1 \leq a$, the cylindrical volume $r_2 \leq b$ is source free, and therefore the fields in this volume are nonsingular.

It can be shown that the axially symmetric term of the $y$-component of the electric field at $r_2 \cong b$ is given by

$$Ey(r_2 \cong b) = \sum_{n=0}^{\infty} \frac{\epsilon_{on}}{B} C_n Q_n J_0(\Gamma_n r_2) \cos(k_{yn} y) \quad \text{(A10)}$$

where $Q_n$ is now given by

$$Q_n = H_0^{(2)}(\Gamma_n r_{1,2}) - \sum_{p=0}^{\infty} \epsilon_{op} J_p^2(\Gamma_n r_{00}) H_p^{(2)}(\Gamma_n R)/J_p(\Gamma_n R)$$

and the axially symmetric term of the $\phi_2$-component of the magnetic field at $r_2 \cong b$ is given by

$$H_\phi(r_2 \cong b) = \sum_{n=0}^{\infty} \frac{\epsilon_{on}}{B} \frac{jk}{Z_0 \Gamma_n} C_n Q_n J_1(\Gamma_n r_2) \cos(k_{yn} y) . \quad \text{(A11)}$$

ACKNOWLEDGMENT

The authors wish to thank Dr. J. Ness, Dr. P. Allen, and other technical staff from MITEC Ltd., Australia, for making available the manufacturing and testing facilities required for accomplishment of the work presented in this paper.

REFERENCES

[1] K. J. Russel, "Microwave power combining techniques," *IEEE Trans. Microwave Theory Tech.*, vol. MTT-27, pp. 472–478, May 1979.
[2] K. Chang and C. Sun, "Millimeter-wave power-combining techniques," *Trans. Microwave Theory Tech.*, vol. MTT-31, pp. 91–107, Feb. 1983.
[3] B. J. Sanders, "Radial combiner runs circles around hybrids," *Microwaves*, pp. 55–58, Nov. 1980.
[4] S. J. Foti *et al.*, "60-way radial combiner uses no isolators," *Microwaves and RF*, pp. 96–118, July 1984.
[5] N. Okubo *et al.*, "A 6 GHz 80-W GaAs FET amplifier with TM-mode cavity power combiner," in *1983 IEEE Int. Microwave Symp. Dig.*, June 1983, pp. 276–278.
[6] P. J. Allen and J. B. Ness, "A hemispherical radial power-waveguide divider/combiner for high power amplifiers," in *IREE Conv. Proc.*, Sydney, 1987, pp. 102–104.
[7] M. E. Bialkowski, "Analysis of disc-type resonator mounts in parallel plate and rectangular waveguides," *Archiv fur Elektronik und Ubertragungstechnik*, AEU, vol. 38, no. 5, pp. 306–311, 1984.
[8] ——, "Analysis of a coaxial-to-waveguide adaptor incorporating a dielectric-coated probe, *IEEE Microwave Guided Wave Lett.*, vol. 1, pp. 211–214, Aug. 1991.
[9] ——, "Modeling of a coaxial waveguide power combining structure," *IEEE Trans. Microwave Theory Tech.*, vol. MTT-34, pp. 937–942, 1986.
[10] R. F. Harrington, *Time Harmonic Electromagnetic Fields.* New York: McGraw-HIll, 1961, Ch. 5.
[11] M. Abramovitz and I. A. Stegun, *Handbook of Mathematical Functions.* New York: Dover, 1965.
[12] R. L. Eisenhart *et al.*, "A useful equivalence for a coaxial-waveguide junction," *IEEE Trans. Microwave Theory Tech.*, vol. MTT-26, pp. 172–174, Mar. 1978.
[13] M. E. Bialkowski and V. P. Waris, "A systematic approach to the design of radial-waveguide dividers/combiners," in *Proc. 1992 Asia-Pacific Microwave Conf.*, Adelaide, pp. 881–884.
[14] V. P. Waris, postgraduate thesis, Univ. Queensland, to be submitted.
[15] M. E. Bialkowski, "Electromagnetic model of a radial-resonator diode mount with off-centered diodes," *IEEE trans. Microwave Theory Tech.*, vol. MTT-37, pp. 1603–1611, Oct. 1989.
[16] M. E. Bialkowski, "Analysis of a planar M-way radial waveguide combiner/divider for the case of arbitrary excitation," in 1993 SBMO Int. Microwave Conf./Brazil Proc., pp. 213–218.

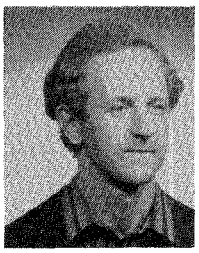

**Marek E. Bialkowski** (SM'88) was born in Sochaczew, Poland, in 1951. He received the M.Eng.Sc. degree in applied mathematics and the Ph.D. degree in electrical engineering, both from the Warsaw Technical University, Warsaw, Poland, in 1974 and 1979, respectively.

In 1977 he joined the Institute of Radioelectronics, Warsaw Technical University, and in 1979 became an Assistant Professor there. In 1981 he was awarded a Postdoctoral Research Fellowship by the Irish Department of Education and spent one year at the University College Dublin carrying out research in the area of microwave circuits. In 1982 he won a Postdoctoral Research Fellowship from the University of Queensland, Brisbane, Australia. During his stay in Brisbane he worked on the modeling of millimeter-wave guiding structures (particularly on waveguide diode mounts). In 1984 he joined the Department of Electrical and Electronic Engineering, James Cook University, Townsville, Australia, as a Lecturer in the field of communications. In 1986 he was promoted to Senior Lecturer. In 1988 he was a Visiting Lecturer in the Department of Electronics and Computer Science, University of Southampton, U.K. He was invited to lecture in the field of antenna theory and design. In 1989 he accepted an appointment as Reader (Associate Professor) in Communications and Electronics in the Department of Electrical Engineering at the University of Queensland, Brisbane, Australia. At present he is the Leader of the Microwave and Antenna Group there. His current research interests include six-port techniques, quasi-optical power combining techniques, modeling of electromagnetically coupled microstrip patch antennas, antennas for mobile satellite communications, near-field/far-field antenna measurements, and industrial applications of microwaves.

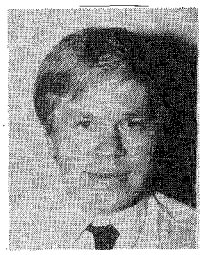

**Vesa P. Waris** (S'91) was born in Pello, Finland, in 1967. He received the B.E. degree from the University of Queensland in 1988.

Since 1989 he has worked for MITEC Ltd. Australia on the L-band Radioastron receiver, phase-locked oscillators and synthesizers, and a 30-GHz receiver using packaged HEMT's. He is currently completing the Master of Engineering Science degree at the University of Queensland.